POLITECNICO DI TORINO
Repository ISTITUZIONALE

Structural topology optimization for plastic-limit behavior of I-beams, considering various beam-column connections

Original
Structural topology optimization for plastic-limit behavior of I-beams, considering various beam-column connections / Grubits, P.; Cucuzza, R.; Habashneh, M.; Domaneschi, M.; Aela, P.; Movahedi Rad, M.. - In: MECHANICS BASED DESIGN OF STRUCTURES AND MACHINES. - ISSN 1539-7734. - 53:4(2025), pp. 2719-2743. [10.1080/15397734.2024.2412757]

Availability:
This version is available at: 11583/2993537 since: 2026-01-13T23:47:30Z

Publisher:
Taylor and Francis

Published
DOI:10.1080/15397734.2024.2412757

Terms of use:

This article is made available under terms and conditions as specified in the corresponding bibliographic description in the repository

Publisher copyright

(Article begins on next page)

11 May 2026

Taylor & Francis
Taylor & Francis Group

Mechanics Based Design of Structures and Machines
An International Journal

ISSN: 1539-7734 (Print) 1539-7742 (Online) Journal homepage: www.tandfonline.com/journals/lmbd20

Structural topology optimization for plastic-limit behavior of I-beams, considering various beam-column connections

Péter Grubits, Raffaele Cucuzza, Muayad Habashneh, Marco Domaneschi, Peyman Aela & Majid Movahedi Rad

To cite this article: Péter Grubits, Raffaele Cucuzza, Muayad Habashneh, Marco Domaneschi, Peyman Aela & Majid Movahedi Rad (2025) Structural topology optimization for plastic-limit behavior of I-beams, considering various beam-column connections, Mechanics Based Design of Structures and Machines, 53:4, 2719-2743, DOI: 10.1080/15397734.2024.2412757

To link to this article: https://doi.org/10.1080/15397734.2024.2412757

© 2024 The Author(s). Published with license by Taylor & Francis Group, LLC

Published online: 10 Oct 2024.

Submit your article to this journal

Article views: 1864

View related articles

View Crossmark data

Citing articles: 26 View citing articles

Full Terms & Conditions of access and use can be found at
https://www.tandfonline.com/action/journalInformation?journalCode=lmbd20

MECHANICS BASED DESIGN OF STRUCTURES AND MACHINES
2025, VOL. 53, NO. 4, 2719–2743
https://doi.org/10.1080/15397734.2024.2412757

Taylor & Francis
Taylor & Francis Group

OPEN ACCESS Check for updates

Structural topology optimization for plastic-limit behavior of I-beams, considering various beam-column connections

Péter Grubits[a], Raffaele Cucuzza[b], Muayad Habashneh[a], Marco Domaneschi[b], Peyman Aela[c], and Majid Movahedi Rad[a]

[a]Department of Structural and Geotechnical Engineering, Széchenyi István University, Győr, Hungary;
[b]Department of Structural, Building and Geotechnical Engineering, Politecnico Di Torino, Torino, Italy;
[c]Department of Building and Real Estate, The Hong Kong Polytechnic University, Kowloon, Hong Kong, China

ABSTRACT

This work proposes topology optimization for steel I-beams, including consideration of bolted beam-column connections with geometric and material nonlinear analysis. The aim is to assess and compare the topological configurations influenced by different connections, examining their stress distribution and rotational stiffness to illustrate the potential of structural optimization. The bi-directional evolutionary structural optimization (BESO) approach is implemented. Furthermore, several bolted steel beam-column configurations were validated based on experimental tests. Subsequently, a series of finite element models were developed, contributing to a comprehensive understanding of the plastic-limit behavior of I-beams under different loading conditions. The proposed method could potentially use a lesser quantity of material while maintaining the same level of structural performance. The results indicate that the implementation of structural topology optimization on I-beams while considering various beam-column connections, yields structural performance similar to that of solid web configurations, achieved through material reduction.

ARTICLE HISTORY
Received 22 April 2024
Accepted 30 September 2024

KEYWORDS
Topology optimization; steel beams; steel connection; nonlinear analysis

1. Introduction

In recent decades, engineers have increasingly directed their attention toward structural optimization, driven by advancements in technology (Cucuzza et al. 2023), environmental considerations (Cucuzza et al. 2024), and economic factors. Structural optimization is presently categorized into three distinct classifications: size, shape, and topological optimization (Christensen and Klarbring 2008; Hsu 1994; Ramm, Maute, and Schwarz 1998). The key aim of this process is to elevate structural performance to the maximum extent possible within predefined constraints, with a specific focus on achieving optimal weight-stiffness and weight-to-resistance ratios (Bendsøe and Sigmund 2004; Rozvany and Lewiński 2014). Elevating the performance of mechanical structures through topology optimization constitutes a complex task, necessitating the automated determination of the optimal material arrangement to ensure efficient utilization (Hao, Liang, and Peigen 2014).

In the last several decades, topology optimization has undergone significant evolution, leading to the development of numerous new computational concepts (Lógó and Ismail 2020). One of the key approaches in topology optimization is the Solid Isotropic Material with Penalization

CONTACT Majid Movahedi Rad majidmr@sze.hu Department of Structural and Geotechnical Engineering, Széchenyi István University, Győr H-9026, Hungary
Communicated by Seonho Cho.

© 2024 The Author(s). Published with license by Taylor & Francis Group, LLC
This is an Open Access article distributed under the terms of the Creative Commons Attribution-NonCommercial-NoDerivatives License (http://creativecommons.org/licenses/by-nc-nd/4.0/), which permits non-commercial re-use, distribution, and reproduction in any medium, provided the original work is properly cited, and is not altered, transformed, or built upon in any way. The terms on which this article has been published allow the posting of the Accepted Manuscript in a repository by the author(s) or with their consent.

(SIMP), in which the material volume serves as the design variable (Bendsøe 1989). Another significant method employed is Evolutionary Structural Optimization (ESO), involving the gradual elimination of inefficient elements to attain an optimal structure (Xie and Steven 1993). In response to the limitations of ESO, the Bi-directional Evolutionary Structural Optimization (BESO) approach was created, capable of both removing material to eliminate low stress and adding material to reduce high stress (Querin, Steven, and Xie 1998). Additionally, other notable methods include the topological derivative method, the level set technique, and the phase field approach (Lógó and Ismail 2020).

The topology optimization is primarily employed in the automotive and aerospace industry (Pucker and Grabe 2011), but also had a major impact on the structural engineering. As a consequence, numerous instances of topology optimization applications have emerged in this field (Blachowski, Tauzowski, and Lógó 2020; Gao, Li, and Ma 2017; Habashneh and Movahedi Rad 2024a; Luo et al. 2014). One of the most fundamental uses includes discrete optimization of truss-like structures, as seen in early applications like transmission tower design through topology and shape optimization (Shea and Smith 2006) or truss optimization method (Torii, Lopez, and Biondini 2012), where the yielding stress and acting forces are treated as random variables. Furthermore, fundamental implementations involve the work of Rozvany, Querin, and Lógó (2004) on the Sequential Element Rejection and Admission (SERA) method to address multiconstraint problems, and Beghini et al.'s research on integrating engineering with architecture through topology optimization (Beghini et al. 2014).

A crucial subfield in civil engineering greatly influenced by topology optimization is the design of steel sections. Initially applying this method, (Kingman, Tsavdaridis, and Toropov 2015) explored two scenarios in which topology optimization proves to be a powerful tool. This study encompasses the structural design of a high-rise structure characterized by geometric complexity and the optimal design of a perforated steel I-section beam. Additionally, recent investigations, as exemplified by the research of Lee, Yang, and Starossek (2012), underscore the efficacy of topological optimization in connection design by systematically assessing the optimal arrangement or reinforcement of materials within designated volumes and design spaces, aiming to maximize stiffness under predefined boundary conditions and stresses. In a similar manner, (Ribeiro et al. 2022) demonstrated the effectiveness of the approach in establishing steel connections. Moreover, (Movahedi Rad, Habashneh, and Lógó 2023) introduced an optimization algorithm, taking into account geometric and material nonlinear imperfect analysis in the cases of deterministic and probabilistic designs.

Recent studies in topology optimization of steel sections have focused on designing perforated I-beams, as seen in (Rocha et al. 2023; Tsavdaridis, Kingman, and Toropov 2015). The findings from these investigations have demonstrated that the optimized design holds the potential to enhance both the stiffness and load-bearing capacity of beams. Although the utilization of perforated I-beams has become more prevalent, traditional I-beams continue to dominate engineering practices (Habashneh et al. 2024; Habashneh and Movahedi Rad 2024b). Moreover, the behavior of global structures is substantially influenced by the semi-rigid connections that link the elements, despite the fact that these connections are frequently assumed to be either rigid or semi-rigid in design practice (Lógó, Kaliszky, and Hjiaj 2006). These aspects together raise the question of whether topological optimization can achieve equivalent load capacity and stiffness for conventional beams under identical conditions, especially when considering the impact of semi-rigid connections. This is particularly relevant because one of the main drawbacks of structural optimization is its reliance on specific boundary conditions and load scenarios.

To address the aforementioned limitation and respond to the posed question, our research distinguishes itself through an innovative approach that integrates topology optimization specifically within the beam-column connection of I-beams. The primary objective is to examine how different connections influence the topology optimization of I-beams and to explore their impact on

the structural behavior of the assemblies, thereby demonstrating the effectiveness and potential of structural optimization in achieving significant material savings without compromising structural performance. To achieve this goal, the proposed work involves the optimization of I-beams utilizing the bi-directional evolutionary structural optimization (BESO) technique, with a focus on various column-beam joints. The finite element models constructed using ABAQUS software (Michael 2009), account for elastic-plastic material behavior and geometric non-linearity, ensuring a precise simulation of realistic conditions. Following the optimization process, a comparative analysis between the results of the optimized beams and conventional I-beams reveals noteworthy advancements. Moreover, our work goes beyond conventional approaches to maximize the accuracy of modeling real-life structural behavior and to provide a more comprehensive understanding of the performance of optimized configurations. This is achieved by introducing initial geometric imperfections to the idealized beams after the optimization process, in alignment with Eurocode standards (European Committee for Standardisation 1993) and building upon previous research (Radwan and Kövesdi 2023; Schillo and Feldmann 2018). As a result, this research makes a noteworthy impact on the field by adopting topology optimization within the domain of beam-column connections. This integration significantly elevates the comprehension and practical application of structural optimization principles in the design of I-beams.

2. Theoretical foundation

This chapter provides an in-depth exploration of the theoretical foundations of topological optimization. Aligned with the central goal of the study, it is imperative to elucidate the principles governing the plastic-limit state. Furthermore, the paper introduces the foundational aspects guiding the consideration of geometric nonlinear analysis.

2.1. Concept of the BESO method

This part provides an elucidation of the Bi-directional Evolutionary Structural Optimization (BESO) approach. This concept involves a systematic process of adding and removing sections to optimize structural performance for a given quantity of material based on the sensitivity levels of individual elements, ultimately achieving the most effective state (Huang and Xie 2010; Yang et al. 1999).

A wide range of techniques, apart from topology optimization approaches, has been developed in the field of structural optimization to achieve highly effective designs, encompassing various advanced algorithms, as exemplified by the work of Kaliszky and Lógó (2003). However, in this research, BESO, recognized as a key technique in topology optimization, was employed due to its unique strengths (Huang, Xie, and Burry 2007). A notable advantage of the BESO over other methods lies in its ability to enhance the precision and convergence of the optimization process by incorporating a filter mechanism to address mesh-dependency problems and checkerboard patterns. This can potentially reduce simulation time and improve the accuracy of the design. Moreover, the BESO also provides freedom in configuring the objective function and adding further design constraints.

In accordance with earlier research (Querin, Steven, and Xie 1998), the topology optimization using the BESO technique is defined as follows:

$$Minimize : C = u^T K u \tag{1}$$

$$Subject\ \ to : V^* = \sum_{i=1}^{N} V_i x_i \tag{2}$$

$$x_i \in \{0, 1\} \tag{3}$$

$$\frac{V^*}{V_0} - V_f \leq 0 \tag{4}$$

where C indicates the structure's compliance, K provides the global stiffens matrix, and u represents the displacements vector. To further clarify, the structure is divided into N elements, where V_i is the volume of a single component, and V^* is the volume of the complete structure. The binary design employs x_i as a variable to indicate whether an element is present or absent, with two possible values: 1 stands for material, and 0 stands for void. Furthermore, the design domain's volume is marked by V_0, and the volume fraction is represented by V_f.

The following formula describes the degree of sensitivity of one component, characterized as the alteration of elastic strain energy:

$$\alpha_i^e = \Delta C_i = \frac{1}{2}\{u_i\}^T[K_i]\{u_i\} \tag{5}$$

where u_i corresponds to the displacement of the individual element, and K_i symbolizes the stiffness matrix, taking into account the sensitivity of void components, which is equal to zero.

Achieving the optimal state of the structure becomes more challenging due to the mesh-dependency problem and the presence of checkerboard patterns. To address these limitations, the BESO method applies a filtering scheme to determine the level of sensitivity of empty components (Huang and Xie 2007). The identification of nodes tasked with preserving the sensitivity of the element is achieved through the utilization of the constant length scale in the filtering scheme, denoted as $r_{\min}$. Derived from the nodes within the sub-domain Ω_i, the enhanced sensitivity number is calculated using the following formula:

$$\alpha_i = \frac{\sum_{j=1}^{k} w(r_{ij})\alpha_j^n}{\sum_{j=1}^{k} w(r_{ij})} \tag{6}$$

where k corresponds to the node's number within the sub-domain and $w(r_{ij})$ is an expression of the linear weight factor, as given by the formula:

$$w(r_{ij}) = r_{\min} - r_{ij} \tag{7}$$

The equation that follows can be used to determine the node's sensitivity:

$$\alpha_j^n = \sum_{i=1}^{M} w_i \alpha_j^e \tag{8}$$

where M devotes the quantity of elements attached to the relevant node, and w_i devotes the element's weight parameter, expressed as:

$$w_i = \frac{1}{M-1}\left(1 - \frac{r_{ij}}{\sum_{i=1}^{M} r_{ij}}\right) \tag{9}$$

where r_{ij} represents the distance in units between the individual element's center and the node. According to the study by Huang et al. (Huang, Xie, and Burry 2007), the optimization process

of the evolution can be stabilized by employing an averaging scheme, defined as:

$$\alpha_i = \frac{\alpha_i^k + \alpha_i^{k-1}}{2} \tag{10}$$

where k stands for the number of the currently performed iteration. Additionally in the next iteration α_i^k will be equel to α_i. The following formula dedicated to the target volume for the subsequent cycle V_{k+1} :

$$V_{k+1} = V_k(1 \pm ER) \tag{11}$$

where ER is a representation for the evolutionary ratio. When the volume satisfies the condition, it will stay constant throughout the subsequent iterations, which are determined by the following equation:

$$V_{k+1} = V^* \tag{12}$$

After completing this process, the components are grouped based on their descending hierarchy of individual sensitivity level. Subsequently, specific conditions will prompt the elimination of solid elements, defined by:

$$\alpha_i \leq \alpha_{del}^{th} \tag{13}$$

while empty elements will only be present if:

$$\alpha_i > \alpha_{add}^{th} \tag{14}$$

where the threshold sensitivity values for removing and adding elements are denoted by α_{del}^{th} and α_{add}^{th}, respectively.

Through the incremental integration and elimination of sections, the BESO approach optimizes a system until the convergence condition is met, specified as follows:

$$error = \frac{\left| \sum_{i=1}^{N} (F_{k-i+1} - F_{k-N-1}) \right|}{\sum_{i=1}^{N} F_{k-i+1}} \leq \tau \tag{15}$$

where F stands for the goal of the function, τ represents the tolerance of the convergence, k is the number of the latest cycle, and N is a quantity in binary that results in continuous adherence for at least ten successful cycles.

2.2. Elasto-plastic BESO analysis

In this study, an elasto-plastic material model for the steel elements was employed in the optimization process. According to this model, the plastic limit state is integrated into the BESO method. The fundamental principle of this analysis is that the component is subjected to a force while assuming this force is continually increasing. In this instance, the expression for the proportional load is:

$$F_i = m_i F_0 \tag{16}$$

where F_0 represents the external forces applied to the structure, and m_i is the load multiplier, a monotonically increasing parameter. As m_i reaches a certain level, the plastic region of the loaded object begins to spread, leading to the development of plastic strains and displacements.

The condition in which an elasto-plastic body undergoes unconstrained plastic deformation when subjected to a constant external force, either entirely or in specific sections, is referred to as

the plastic limit condition. In this case, the plastic limit load can be expressed as follows:

$$F_p = m_p F_0 \tag{17}$$

where m_p represents the load multiplier, indicating the component undergoing plastic deformation.

At this limit condition, equilibrium equations are employed because the internal and external forces ensure the static equilibrium of the structure. Additionally, the yield criteria are met by considering the stress σ_{ij} within an object. This involves maintaining quasi-static equilibrium under the plastic limit load, as well as taking into account the statistically acceptable level of stress σ_{ij}^s and the force $F_{i,s} = m_s F_0$, defined as:

$$f\left(\sigma_{ij}^s, k\right) \leq 0 \tag{18}$$

where k represents the plastic properties associated with a defined material. Taking into consideration a deformable component characterized by the volume V and the area of applied load S_q, virtual velocities are utilized to compute stress and force distributions, as expressed in the following formulation:

$$\int_V \sigma_{ij}\dot{\varepsilon}_{ij} dV = m_p \int_{S_q} F_0 v_i dS \tag{19}$$

$$\int_V \sigma_{ij}^s \dot{\varepsilon}_{ij} dV = m_s \int_{S_q} F_0 v_i dS \tag{20}$$

where $\dot{\varepsilon}_{ij}$ is standing for strain rate and v_i is standing for the velocities. The result of subtracting Eqs. (19) and (20) is:

$$\int_V \left(\sigma_{ij} - \sigma_{ij}^s\right)\dot{\varepsilon}_{ij} dV = \left(m_p - m_s\right) \int_{S_q} F_0 v_i dS \tag{21}$$

In consideration of the yield surface's convexity and the normality rule, which translates to a set of conditions governing the material's yielding behavior:

$$\left(\sigma_{ij} - \sigma_{ij}^s\right)\dot{\varepsilon}_{ij} \geq 0 \tag{22}$$

therefore, as illustrated in Fig. 1, the following formula is obtained:

$$\left(m_p - m_s\right) \int_{S_q} F_0 v_i dS \geq 0 \tag{23}$$

The Eq. (23) demonstrates that the component's velocities are influenced by external forces. Furthermore, the concept of the plastic limit condition incorporates the material's inability to perform negative work (Movahedi Rad, Habashneh, and Lógó 2021). Consequently, the following equation applies:

$$m_s - m_p \leq 0 \tag{24}$$

The plastic limit multiplier m_p can be integrated into the optimization process without adding significant mathematical complexity. In this context, the topology optimization using BESO method is defined as:

$$Minimize : C = u^T K u \tag{25}$$

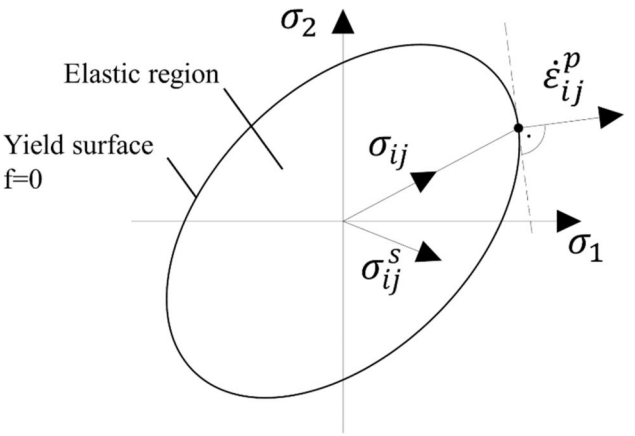

Figure 1. The von Mises yield surface under plane stress conditions.

$$Subject\ \ to: V^* = \sum_{i=1}^{N} V_i x_i \tag{26}$$

$$x_i \in \{0, 1\} \tag{27}$$

$$\frac{V^*}{V_0} - V_f \leq 0 \tag{28}$$

$$m_s - m_p \leq 0 \tag{29}$$

The constraint $m_s - m_p \leq 0$, incorporated into the optimization process, ensures the viability and reliability of the solution in scenarios involving plastic strains. Consequently, this method is well-suited for optimizing elastic-plastic structures that experience plastic deformation under high load intensity. Conversely, the aforementioned constraint is intentionally omitted in situations that exhibit elastic solutions, particularly at lower load ratios. Thus, this method also effectively accommodates elastic behavior.

2.3. Geometric nonlinear analysis

In this study, geometric nonlinearity was utilized during the analysis to take into consideration the effects of large deformations. This solution allows the precise prediction of the behavior of different steel elements incorporated in finite element simulation. The Piola-Kirchhoff matrix and the Green-Lagrange matrix were employed to assess the connection between stress and strain during the calculation (Bathe 2014). Consequently, the Green-Lagrange strain is expressed as follows:

$$\eta_{ij} = \frac{1}{2}\left(u_{i,j} + u_{j,i} + u_{k,i}u_{k,j}\right) \tag{30}$$

where parameter u is representing the point-wise displacement. For subsequent application, the following relation is relevant:

$$d\boldsymbol{\eta} = \boldsymbol{B}(\boldsymbol{U})d\boldsymbol{U} \tag{31}$$

where $\boldsymbol{B}$ represents the finite element matrix that relates changes in displacement $d\boldsymbol{U}$ to changes in strain $d\boldsymbol{\eta}$. In this context, $\boldsymbol{U}$ denotes the displacement matrix of the finite element, encompassing the displacements of all the nodes within that element.

Regarding Piola-Kirchhoff and Green-Lagrange strains, the linear Hooke's law is expressed as:

$$s_{ij} = D^{e}_{ijkl}\eta_{kl} \tag{32}$$

Where D^{e}_{ijkl} indicates the constitutive tensor of the element, denoted by e, and η_{kl} represents the Green-Lagrange strains. When modeling elements with intermediate densities using the power law approach, Hooke's law is given by:

$$s_{ij} = (p_e)^{p} D^{0}_{ijkl}\eta_{kl} \tag{33}$$

where p is the penalization power and D^{0}_{ijkl} stands for the constitutive matrix for a homogeneous isotropic material. The residual, characterized by deviation from the attained equilibrium, is expressed through the following exclusion:

$$\boldsymbol{R}(\boldsymbol{U}) = \boldsymbol{P} - \int_{V} \boldsymbol{B}^{T}\boldsymbol{s}dV \tag{34}$$

where $\boldsymbol{P}$ represents the applied external force matrix and $\boldsymbol{s}$ denotes the Piola-Kirchhoff stress matrix. Equilibrium can be achieved when the residual matrix equals zero, which can be determined using the Newton-Raphson method through an iterative process, defined as:

$$\boldsymbol{K}_{T} = -\frac{\partial \boldsymbol{R}}{\partial \boldsymbol{U}} \tag{35}$$

where $\boldsymbol{K}_{T}$ is standing for the stiffness matrix.

3. Finite element simulation

In this study, the ABAQUS software was employed to model the examined specimens (Michael 2009). A comprehensive investigation was conducted, incorporating both perfect geometrical and material nonlinear analyses (GMNA). Additionally, at a later stage, GMNA was extended by introducing initial global geometric imperfections (GMNIA). The results of the numerical simulation were validated through experimental tests in three cases (web cleat, angle flange cleat, combined). Different types of connections were also added to the research to cover a broader range of tests.

The optimization algorithm proposed in this study utilizes ABAQUS for finite element analysis in each iteration. The results obtained from the FEA form the basis for the code, implementing the BESO method. In summary, the code methodically shapes and refines the designated segment over iterations, ultimately reaching an ideal configuration. The entire process is depicted in Fig. 2.

3.1. Performing finite element analysis

The first phase of the study involves simulating the behavior of regular steel beams with various types of column connections. ABAQUS, a commercial general finite element software, was utilized for this purpose.

To characterize the behavior of beams based on different column connections, comprehensive 3D models were developed, incorporating various joint components. In general, these parts use hexahedral-dominated solid 3D elements with 8 nodes and reduced integration (C3D8R). Additionally, the analysis incorporates both geometric and material nonlinearity to capture the complex behavior exhibited by the steel. In addressing the nonlinear challenge posed by significant deformation, the Newton-Raphson technique is utilized to identify static equilibrium states throughout the unstable phase of the response (Michael 2009).

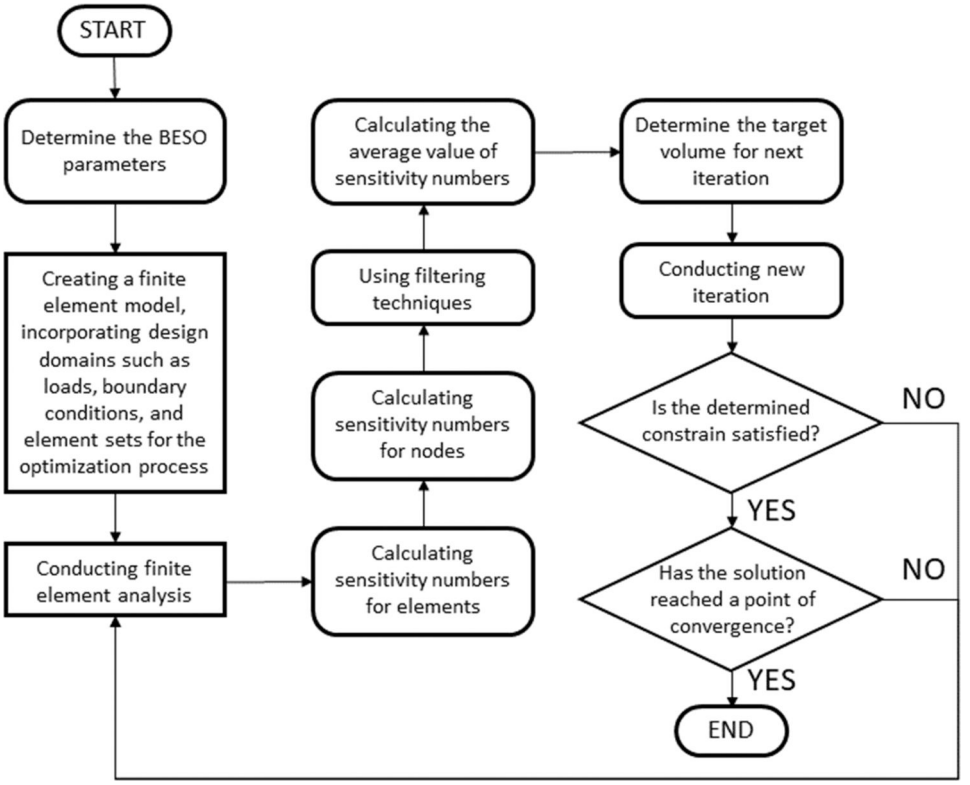

Figure 2. Process of BESO.

For the modeling of the contact between bolts angels, and plates "surface-to-surface" interactions were utilized. The contact property incorporates tangential behavior with a friction coefficient of 0.3 and normal behavior with the "hard" contact option (Michael 2009).

3.2. Geometric imperfection

In a subsequent phase of the study, the geometric and material nonlinear analysis incorporated an initial imperfection. These imperfections help elucidate deviations from perfect geometry observed in real structures. Including these aspects in finite element analysis enhances the accuracy and precision of predictions regarding the structural behavior.

For the analysis, the initial geometric imperfection was determined as the eigenvector of the first eigenmode identified through the linear buckling analysis (LBA) conducted in ABAQUS (Michael 2009). The buckling mode observed corresponded to lateral torsion in every configuration, albeit with varying values of elastic critical loads. It is noteworthy to mention that the main objective of this study is not to determine the smallest value of the collapsing load; instead, this work focuses on assessing the impact of geometric imperfections on the behavior of the optimized beams.

4. Steel beam-column joint configurations

In this research, a total of 5 configurations were tested, of which the first three are validated trough the experimental test of Yang and Tan (2013). All these joints exhibit semi-rigid behavior;

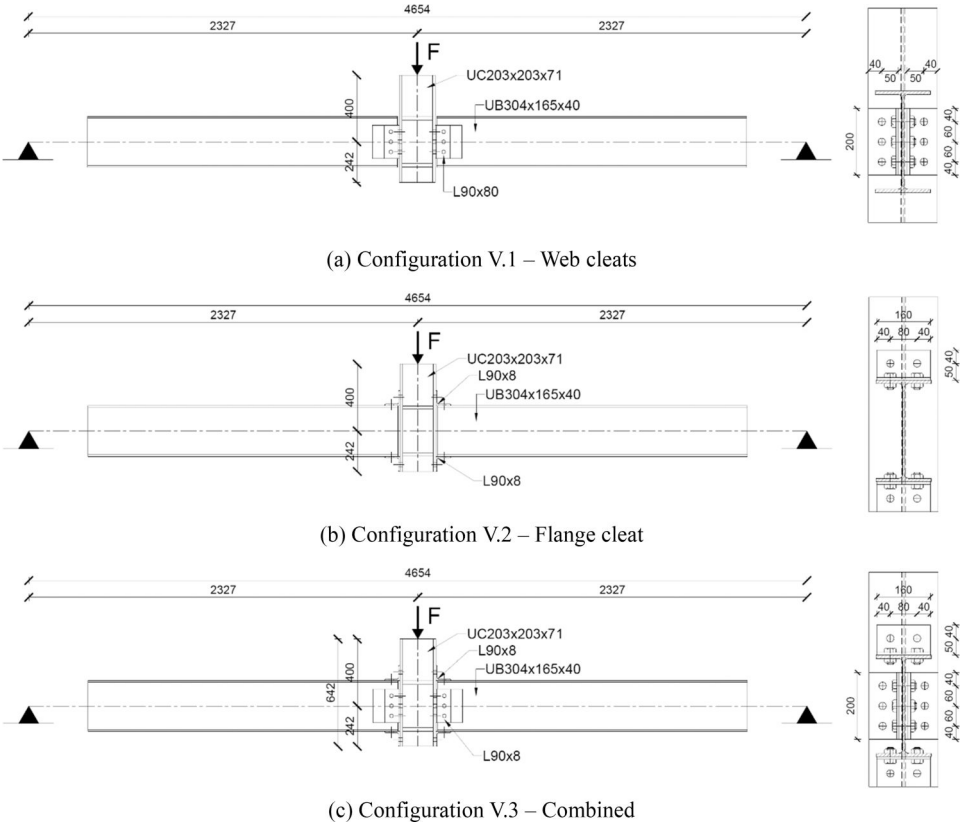

Figure 3. The configurations based on experimental tests.

however, based on previous experience (Ivanyi and Baniotopoulos 2000), their stiffness classification according to the Eurocode (European Committee for Standardisation 2005b) is closer to that of flexible category. Furthermore, two different stiffer configurations were investigated to explore the effect of the optimized beam on stress distribution and rotational stiffness of the joint. These include a fully welded connection and an extended plate connection, where the cross-sections of the beam are the same as those used in the experimental test by Yang and Tan (2013).

4.1. Configurations based on experimental tests

In the first part of the study, the maximum load-bearing capacity of three beam-column assemblies was calculated, with validation referring to the work of Yang and Tan (2013). The examined connections include web cleats, flange cleats, and combinations of these two, as illustrated in Fig. 3, incorporated with components, loads, and boundary conditions. Based on previous experimental tests, all three connections can be classified as semi-rigid (Ivanyi and Baniotopoulos 2000). The main characteristics are detailed in Table 1, while the principal material properties, specified in accordance with the EN1993-1-1 (European Committee for Standardisation 2005a) and EN1993-1-8 (European Committee for Standardisation 2005b) standards, are provided in Table 2. The cross-section of the optimized steel I-beams is UB305x165x40, as investigated in the study of Yang and Tan (2013). The beam has a flange width of 165 mm and an overall depth of 304 mm. In terms of nominal thicknesses, the flange is 10.2 mm, and the web is 6.1 mm thick.

Table 1. Main characteristics of the validated configurations.

Configuration ID	Connection type	Beam	Column	Angle	Bolt
V.1	Web cleats	UB305x165x40 – S355	UC203x203x71 – S355	L90x8 – S275	M20 – 8.8
V.2	Flange cleats	UB305x165x40 – S355	UC203x203x71 – S355	L90x8 – S275	M20 – 8.8
V.3	Combined	UB305x165x40 – S355	UC203x203x71 – S355	L90x8 – S275	M20 – 8.8

Table 2. Main material properties of the steel elements.

Material grade	Modulus of elasticity (N/mm^2)	Yield strength (N/mm^2)	Ultimate strength (N/mm^2)
S355	210,000	355	510
S275	210,000	275	430
8.8	210,000	640	800

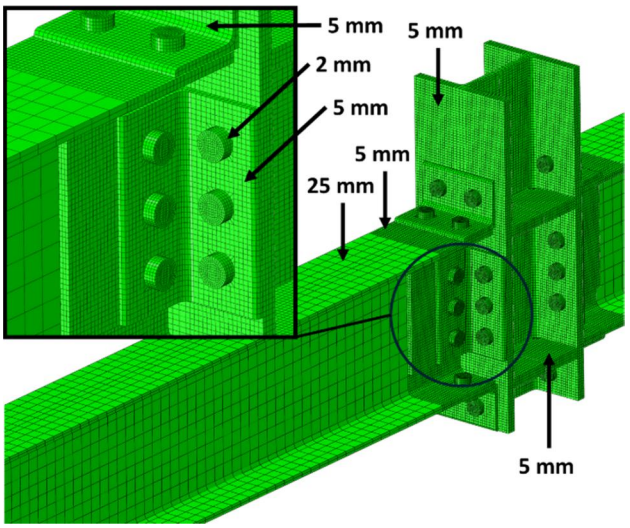

Figure 4. The typical mesh structure of the numerical models.

As discussed in previous chapters, the models were constructed using hexahedral-dominated solid 3D elements with eight nodes and reduced integration (C3D8R). To balance computational efficiency with accuracy, varying mesh sizes were applied to the structural elements. Specifically, a general mesh size of 5 mm was employed for the angles, plates, the column, and the section of the beam near the connection, while a coarser 25 mm mesh was applied to the remaining portion of the beam. Additionally, the bolts were modeled with a finer 2 mm mesh. The mesh structure is illustrated in Fig. 4, using the configuration V.3 as an example.

It is important to note that the numerical models employed for optimization in this study, as detailed in a subsequent chapter, adhere to the same specifications outlined in this section. These characteristics include cross-sectional geometry, material properties, and mesh structure.

The initial primary objective was to validate the mentioned beam-column connections, which subsequently served as various boundary conditions in the optimization process. The results from the FE simulation are presented in Table 3 and compared with those from the experimental tests. In all three cases, the load capacity associated with the ultimate displacement is within the acceptable 10% error margin according to the work of Yang and Tan (2013). Additionally, the von Mises stresses related to the ultimate load are illustrated in Fig. 5.

Table 3. Experimental and numerical results of the validated configurations.

		Experimental test		Numerical test	
Configuration ID	Connection type	Vertical load F (kN)	Displacement (mm)	Vertical load F (kN)	Displacement (mm)
V.1	Web cleats	119.0	367	110.9	368
V.2	Flange cleats	44.8	243	46.7	236
V.3	Combined	77.5	233	71.3	227

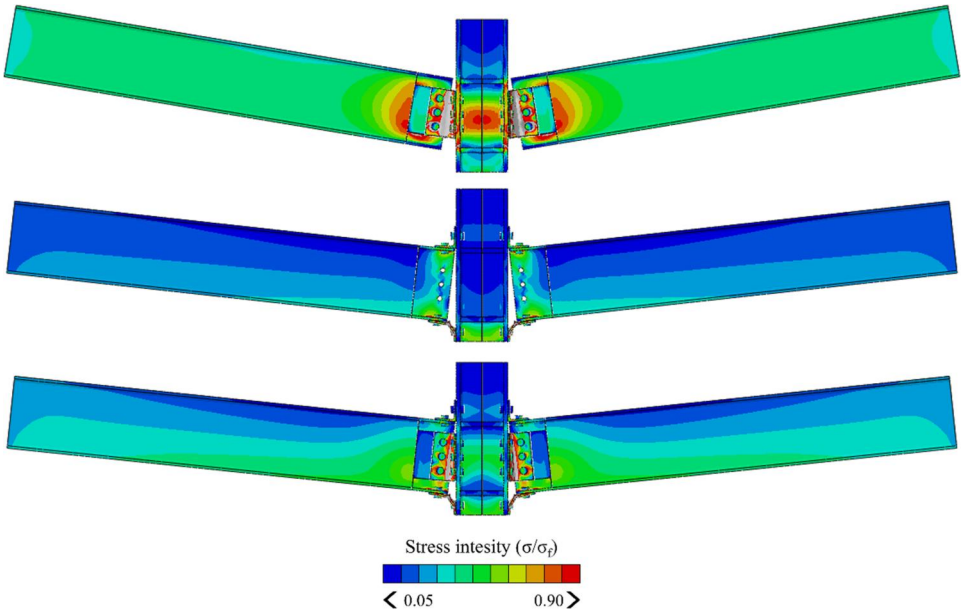

Figure 5. The Resulting Von Mises stresses in the validated numerical models.

4.2. Configurations for structural optimization

In the context of topological optimization, a more realistic set-up, as illustrated in Fig. 6, was utilized, where beams were positioned between two columns. The parameter "F" marked on the pictures indicates the position of the applied load. In these configurations, the different beam-column joints served as various boundary conditions. Two additional setups, extended end plate, and fully welded beam-column connections, were added to the three semi-rigid models. These setups, based on previous experience (Ivanyi and Baniotopoulos 2000) and the numerical results, exhibit much more rigid behavior.

In the configurations devised for the presented optimization process, the parameters introduced in the validation procedure were employed. These include the cross-sections of the different parts, the material properties and the mesh structure. In addition, the FEA settings are consistent between the validated model and the models presented here.

In the second phase of the investigation, the model's initial geometric imperfection was utilized. For this purpose, eigenvectors corresponding to the first eigenvalue obtained during the linear buckling analysis (LBA) were employed. The amplitude of the imperfection was set to L/1000, where L represents the length of the I-beam. The ultimate loads obtained are presented in Table 4, including values for configurations both without imperfections and with imperfections.

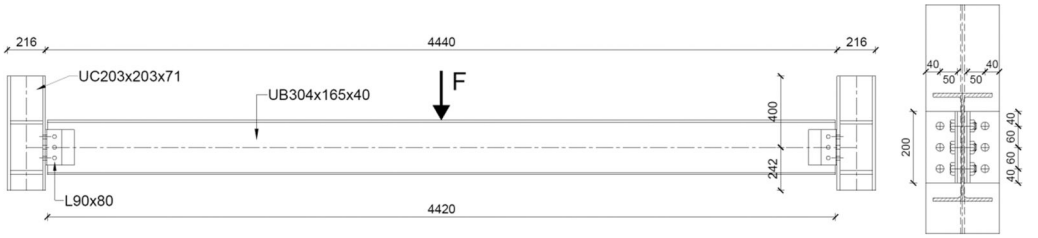

(a) Configuration O.1 – Web cleats

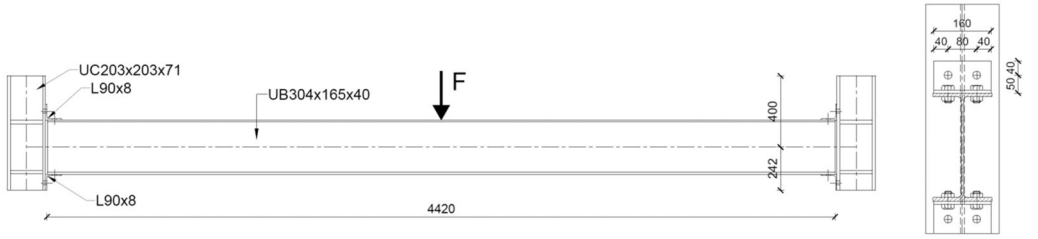

(b) Configuration O.2 – Flange cleats

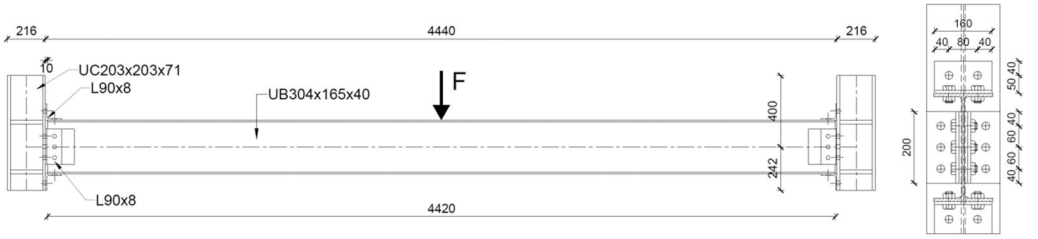

(c) Configuration O.3 – Combined

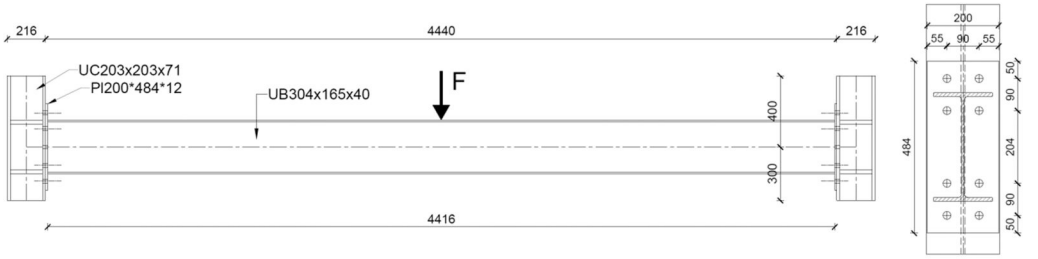

(d) Configuration O.4 – Extended end-plate

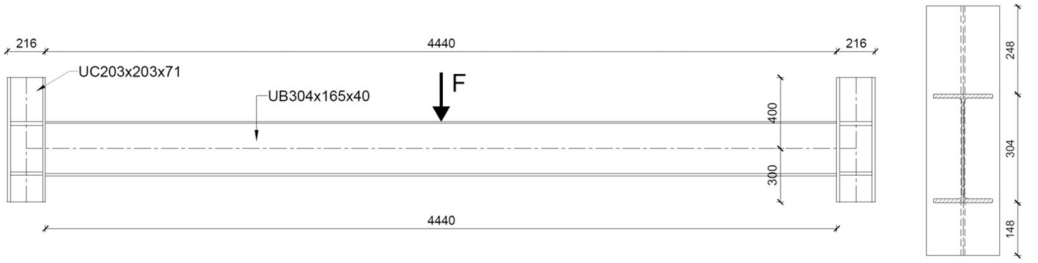

(e) Configuration O.5 – Welded

Figure 6. The configurations used for the optimization process.

Table 4. Ultimate loads of the configurations used for optimization process.

Configuration ID	Connection type	Ultimate load without imperfection F_u (kN)	Ultimate load with imperfection F_u (kN)
O.1	Web cleats	245	136
O.2	Flange cleats	272	144
O.3	Combined	287	162
O.4	Extended end-plate	310	220
O.5	Welded	339	282

Table 5. Values of the applied load (F_0), the ultimate load multiplier (m_p) and elastic load multiplier ($m_{s,i}$).

		Without imperfection				With imperfection			
Configuration ID	F_0 (kN)	m_p	$m_{s,1}$	$m_{s,2}$	$m_{s,3}$	m_p	$m_{s,1}$	$m_{s,2}$	$m_{s,3}$
O.1	100	2.45	0.61	1.23	1.84	1.36	0.34	0.68	1.02
O.2		2.72	0.68	1.36	2.04	1.44	0.36	0.72	1.08
O.3		2.87	0.72	1.44	2.15	1.62	0.41	0.81	1.22
O.4		3.10	0.78	1.55	2.33	2.20	0.55	1.10	1.65
O.5		3.39	0.85	1.70	2.54	2.82	0.71	1.41	2.12

Table 6. The computational time of the optimization process.

Configuration ID	Connection type	CPU time required for the optimization process (seconds)
O.1	Web cleats	2172
O.2	Flange cleats	1892
O.3	Combined	3132
O.4	Extended end-plate	1597
O.5	Welded	1390

5. Implementation of the proposed optimization approach

This section is dedicated to implementing the proposed optimization methodology, with a particular emphasis on minimizing the quantity of material. During the process, the optimized shape of the steel I-beam's web for the earlier presented configurations was determined, taking into account the values of the ultimate loads. In these load scenarios, each setup experienced plastic deformation. Subsequently, a comparison was conducted between configurations with regular I-beams and optimized I-beams, examining stress distribution and rotational stiffness, which constituted the primary objectives of the research. Finally, geometrical imperfections were applied to the structural assemblies, and the previously analyzed parameters were reevaluated.

To compare the stress distribution across the configurations, the concept of the plastic load multiplier was employed. For clarity, different load intensities were applied to the structures, where the load value $F_{s,i}$ equals the initially applied load F_0 multiplied by the elastic load multiplier $m_{s,i}$. The three $m_{s,i}$ considered are 25%, 50%, and 75% of the ultimate load multiplier m_p for each configuration, corresponding to the levels at which the structures reach the plastic limit state, where the ultimate load is defined as $F_u = m_p F_0$. The parameters are presented in Table 5.

For the optimization process, an Intel® Core™ i5–11320 CPU, operating at 3.20 GHz with 16.0 GB of RAM, was utilized within a personal computer system. The computational efficiency of the proposed approach is assessed through the CPU times for the simulations, which are presented in Table 6.

5.1. Considering the optimized shape of the beams

In this section, the outcomes of the proposed topology optimization method are contrasted with those of beams where the webs form a continuum. During the first phase of the process, BESO

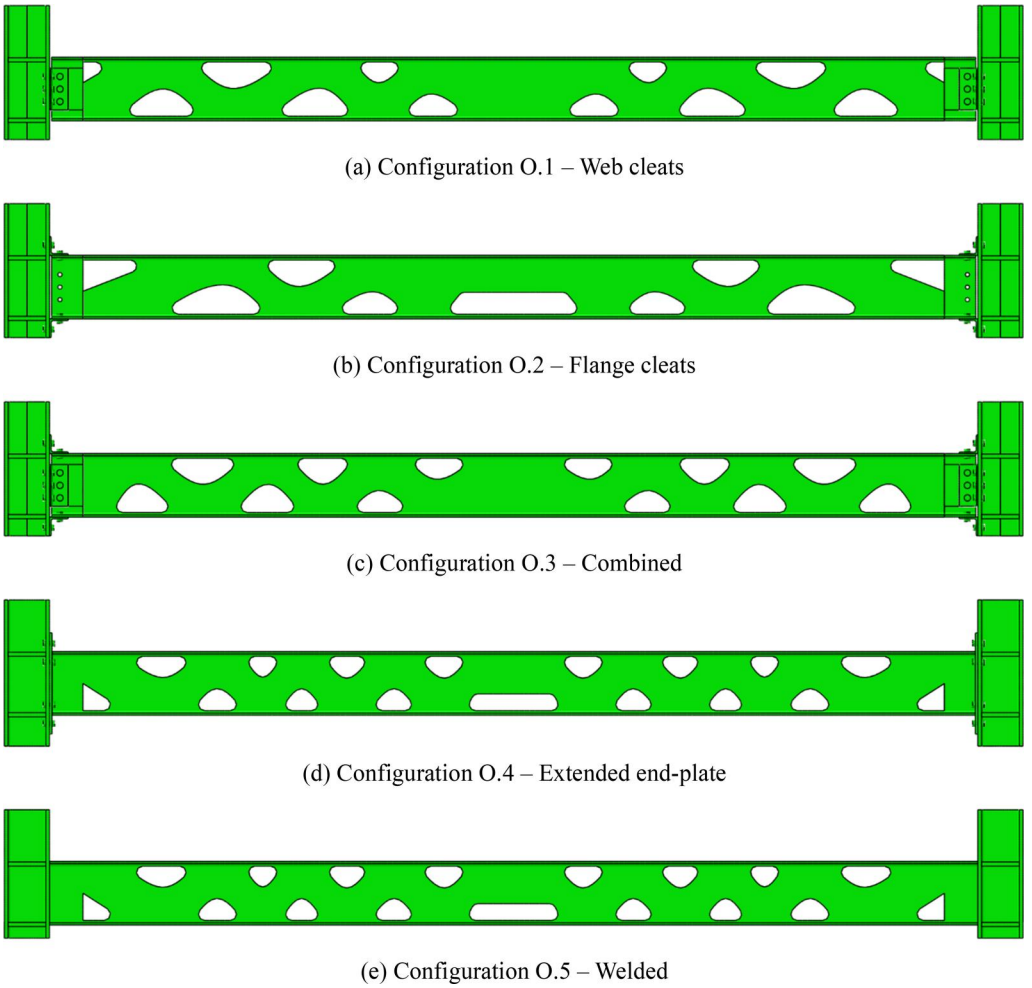

Figure 7. The resulted topology shapes of the different configurations.

was applied, considering the same ultimate load value for different configurations as presented in Table 4, without incorporating the initial geometric imperfections of the I-beams. The obtained topological shapes are presented in Fig. 7. A volume fraction of 70% was set for the topology optimization process.

From the result presented in Fig. 7, it can be observed that the optimization process consistently resulted in a truss-type structural design in each case. However, the geometry of the optimized shapes varies based on the connections between the beams and columns, with variations expected in configurations O.4 and O.5. The similarity in behavior and stiffness of the two joints in question is the reason for this, serving as nearly identical boundary conditions for the beam during the optimization process. Additionally, it can be observed that, in the case of O.1, O.2, and O.3, due to the less rigid behaviors of the joints, the moment at the end of the beams is relatively low, resulting in a concentration of material distribution more in the middle of the beams. Moreover, it's significant to mention that the topology pattern of configuration O.3 also combines the shape of O.1 and O.3.

It is important to emphasize that while this research primarily focuses on the topology optimization of I-beams from a design perspective, ensuring the manufacturability of the optimized

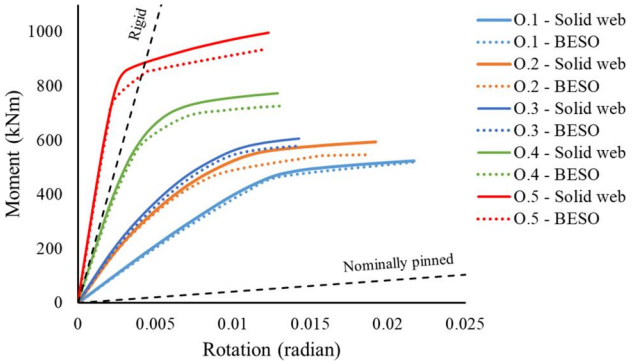

Figure 8. Moment-rotation relations of the configurations without considering geometric imperfections.

Table 7. Comparison between the stress distribution without initial geometric imperfection by considering $F_1 = m_{s,1}.F_0$

Configuration ID	Solid web I-beam	Topology optimization
O.1		
O.2		
O.3		
O.4		
O.5		

structural elements is also a critical objective. Advances in additive manufacturing technologies have enabled the production of metal structures with large and complex topologies (Fernández et al. 2021; Ibhadode et al. 2023). Among the various techniques, wire-and-arc additive manufacturing (Laghi et al. 2023) is particularly suited for fabricating the optimized beams proposed in this study.

After the optimization process, additional simulations were conducted using the load parameters defined in Table 5 as the external load for the different configurations. Tables 7–9 display

Table 8. Comparison between the stress distribution without initial geometric imperfection by considering $F_2 = m_{s,2} \cdot F_0$

Configuration ID	Solid web I-beam	Topology optimization
O.1	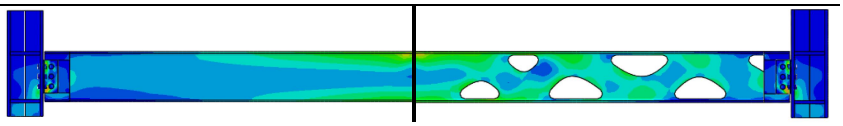	
O.2	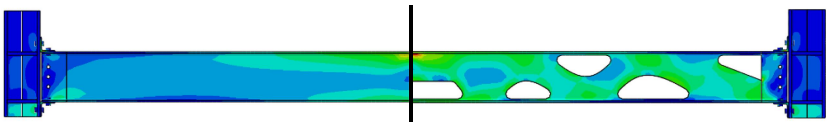	
O.3	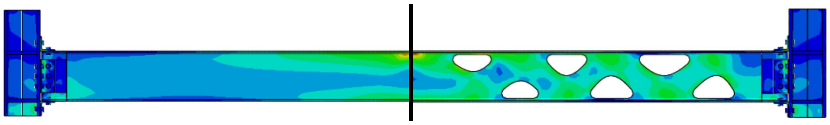	
O.4	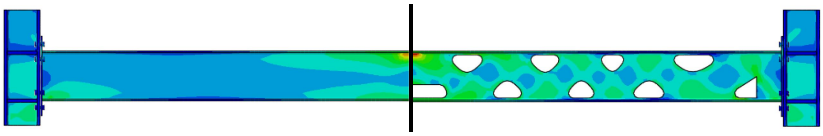	
O.5	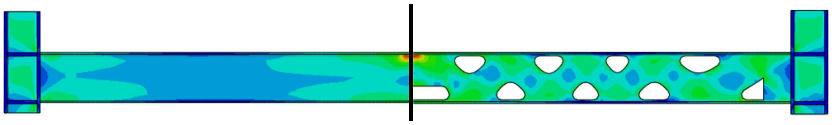	

the von Mises stresses obtained by employing plastic-limit analysis for various configurations. The plot of stress distributions provides insights into the behavior of the structural elements.

After examining the results presented in Tables 7–9, it is noticeable that the stress distributions in the case of the optimized configurations are generally more evenly distributed along the I-beam web. This observation aligns with the principles of the BESO method employed. Similar quantities of material exceeding yielding are detected in all scenarios, localized in the load area of each assembly.

Finally, a comparison of the rotational stiffness of the configurations was conducted, evaluating both solid web beam assemblies and their optimized counterparts. These results are depicted in Fig. 8, where the classification boundaries according to EN1993-1-8 can be observed. Evidently, the optimization process had a slight impact on the rotational stiffness of the connections. However, upon closer examination, the deviation in the maximum moments that can be absorbed by the joints, corresponding to the moment resistance of the connection, was found to be less than 10% in each case, as shown in Table 10. Remarkably, the initial rotational stiffness for the flexible section is assumed to be consistent, whether it's beams with a solid web or beams with an optimized web. Therefore, within the elastic range, the structural behavior and performance of conventional and idealized setups are nearly identical, with the maximum deviation remaining below 4%, as illustrated in Table 11. Moreover, the behavior of the configurations aligns with the outcomes of previous experiments.

Table 9. Comparison between the stress distribution without initial geometric imperfection by considering $F_3 = m_{s,3}$. F_0

Configuration ID	Solid web I-beam	Topology optimization
O.1	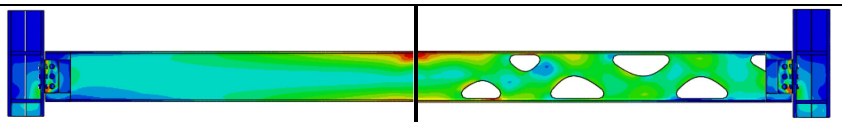	
O.2	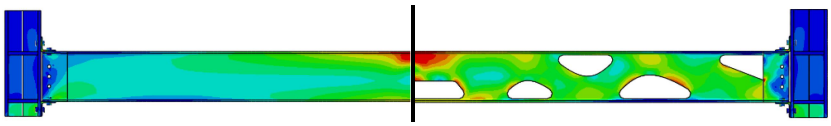	
O.3	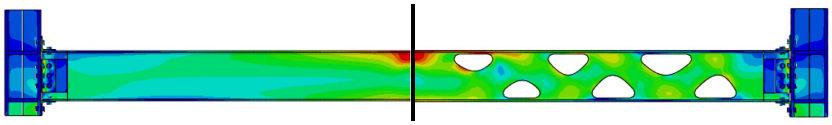	
O.4	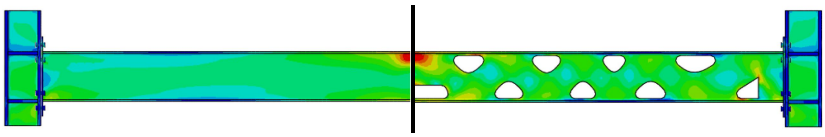	
O.5	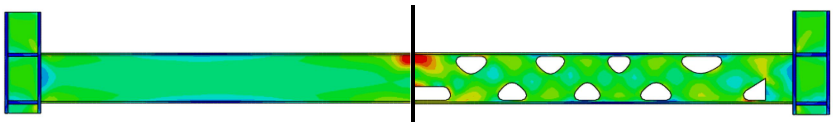	

5.2. Considering the geometric imperfection

In the final part of the study, initial geometric imperfections were introduced to the beams in the previously described configurations to enhance the accuracy of simulating real-life structural behavior and to provide a greater understanding of the performance of the optimized setups. Additional research was conducted on the stress distribution of the I-beams and on the rotation-moment relations of the joints, and a comparison was drawn between the standard I-beams and the topology-optimized I-beams. In this section, identical topology shapes, as depicted in Fig. 7, were employed.

The von Mises stresses, obtained through simulations considering initial geometric imperfections, are illustrated in Tables 12–14, following the concept of the plastic limit state. After conducting the linear buckling analysis (LBA), the amplitude of the eigenmode corresponding to the first eigenvalue was set to $L/1000$ as the initial imperfection for the beam, where L represents the length of the I-beam.

During the simulations, lateral buckling of the I-beam due to geometric imperfections occurred in each configuration. Consequently, both types of assemblies, with solid-web I-beams and optimized-shape I-beams, exhibited lower load capacity and stress intensity when imperfections were considered. Generally, the stress distribution, as shown in Tables 12–14, closely resembled the results obtained without imperfections, illustrated in Tables 7–9. In this case as well, stress along

Table 10. Deviation in the maximum moment of the connections without geometric imperfection.

	Maximum moment (kNm)		
Configuration ID	Solid web	BESO	Deviation
O.1	524	519	0.95%
O.2	593	546	7.93%
O.3	605	577	4.63%
O.4	773	726	6.08%
O.5	996	933	6.33%

Table 11. Deviation in the initial rotational stiffness of the connection without geometric imperfection.

	Initial rotational stiffness (kNm/rad)		
Configuration ID	Solid web	BESO	Deviation
O.1	39,564	38,642	2.33%
O.2	74,302	72,433	2.52%
O.3	80,462	77,527	3.65%
O.4	169,938	164,001	3.49%
O.5	355,200	351,238	1.12%

Table 12. Comparison between the stress distribution with initial geometric imperfection by considering $F_1 = m_{s,1}$. F_0

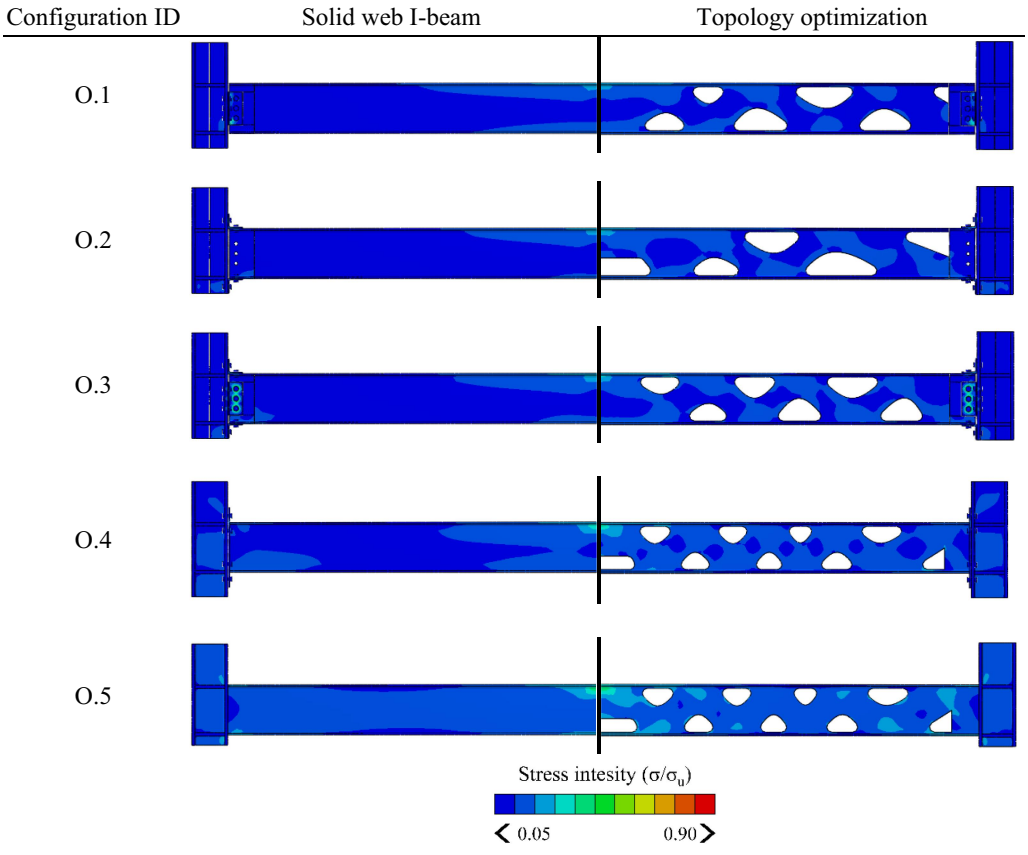

Table 13. Comparison between the stress distribution with initial geometric imperfection by considering $F_2 = m_{s,2}.\ F_0$

Configuration ID	Solid web I-beam	Topology optimization
O.1	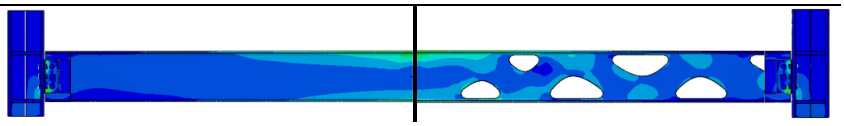	
O.2	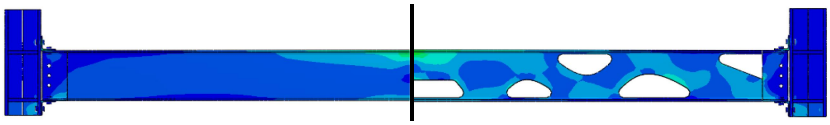	
O.3	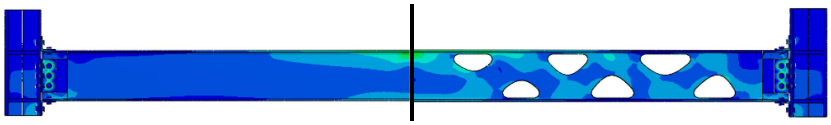	
O.4	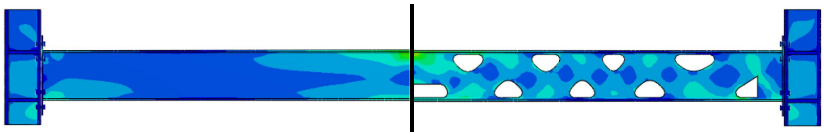	
O.5	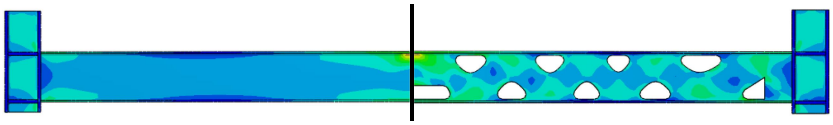	

the topology-optimized web of the beams was more evenly balanced, achieving consistent structural behavior and fulfilling the main objective of the BESO method.

As one of the primary goals of the study, the rotational stiffness of the configurations, considering initial geometric imperfections of the I-beams, was compared to each other. The obtained results are depicted in Fig. 9, where, once again, the classification boundaries according to EN1993-1-8 (European Committee for Standardisation 2005b) standard are visible. Due to their initial buckling shape, the I-beams underwent lateral buckling deformations early in the loading history within the elastic range. This phenomenon significantly compromised the structural stability of the assemblies. The influence of these assumed buckling modes extends throughout the entire configuration, resulting in changes to its structural behavior, specifically contributing to a decrease in the connection's load-bearing capacity. Consequently, the maximum moment absorption capability of the joints is lower than the values presented in Table 10 from the preceding section. Despite topology optimization influencing the rotation-moment relations to some extent, the deviation in moment resistance of the connections across configurations remains below 10%, as illustrated in Table 15. Furthermore, there is no significant disparity in the initial rotational stiffness values between the optimized beams and the solid web beam assemblies, with the maximum deviation remaining below 5%, as shown in Table 16.

Table 14. Comparison between the stress distribution with initial geometric imperfection by considering $F_3 = m_{s3}.\ F_0$

Configuration ID	Solid web I-beam	Topology optimization
O.1	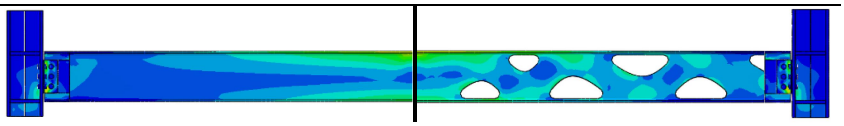	
O.2	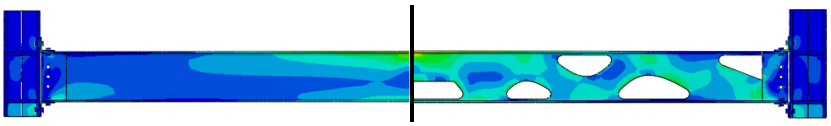	
O.3	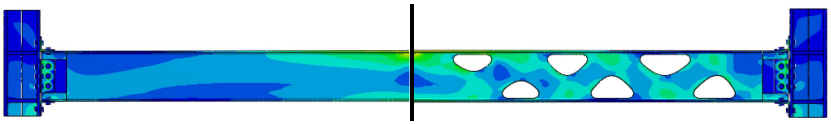	
O.4	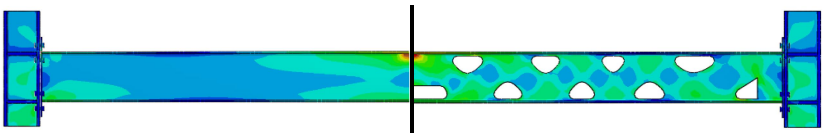	
O.5	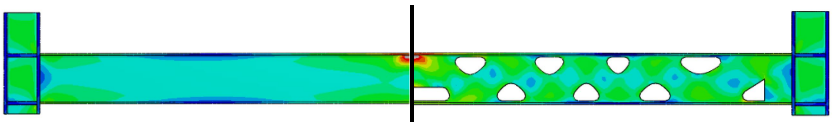	

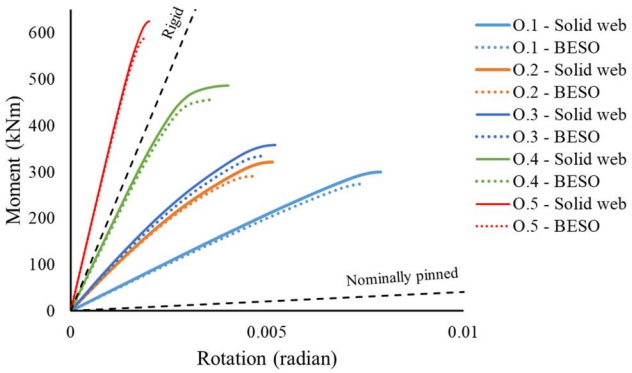

Figure 9. Moment-rotation relations of the configurations considering geometric imperfections.

Table 15. Deviation in the maximum moment of the connections with geometric imperfection.

	Maximum moment (kNm)		
Configuration ID	Solid web	BESO	Deviation
O.1	300	274	8.67%
O.2	322	291	9.63%
O.3	358	334	6.70%
O.4	487	455	6.57%
O.5	625	582	6.88%

Table 16. Deviation in the initial rotational stiffness of the connection with geometric imperfection.

	Initial rotational stiffness (kNm/rad)		
Configuration ID	Solid web	BESO	Deviation
O.1	39,387	37,960	3.62%
O.2	72,909	71,227	2.31%
O.3	76,802	73,073	4.85%
O.4	166,862	161,683	3.10%
O.5	340,907	336,376	1.33%

6. Conclusion

In this paper, a comprehensive geometric and material nonlinear analysis of five different beam-column configurations incorporating topology optimization of the designated section of the inspected beams was conducted. One of the biggest disadvantages of structural topology optimization is that the structure is optimized for a specific boundary condition and load. Consequently, in this paper, the optimized shape of the same I-beam was produced considering different types of connections, serving as various boundary conditions. As a result, we obtained different layouts, with the exception of one case, due to the similar behavior of the affected assemblies.

The primary objective of this investigation was to compare the structural behavior of conventional beams and optimized beams. To achieve this goal, in the first part of the paper, three different joints were validated based on previous experimental tests. After this procedure, a more realistic configuration was introduced proceeding from the results of the validation, and additionally, two more connection types were added to the simulations to broaden the investigation spectrum. Using the powerful BESO algorithm presented in this study, the optimized shapes of the I-beams associated with various connections were created. Finally, the behavior of the optimized setups was compared to the regular ones through stress distribution and rotational stiffness.

The suggested method aimed to optimize the stress intensities and guarantee, with acceptable deviation, the same structural performance with a smaller quantity of material by taking the plastic load multiplier into consideration. This application demonstrated the efficacy and rationality of the method, resulting in encouraging findings that are reported in this study. The optimized configurations showed nearly the same rotation-moment relations with no relevant deviation in the peak moment that the joints can absorb, both with and without incorporating initial geometric imperfections of the I-beams. In every instance, this margin was less than the permissible 10%. Remarkably, there was a negligible difference in the initial rotational stiffness of the joints between the ordinary and optimized assemblies, with a maximum deviation of 4.85%.

In conclusion, this paper represents a relevant improvement in the design methodologies for beams considering different types of column-beam connections. The results obtained from the simulations verify that the proposed optimization method has great potential to provide an economical design with savings in the quantity of material using the concept of the plastic limit state.

Authors contributions

Péter Grubits: Writing – Original Draft, Investigation, Visualization, Software, **Rafaelle Cucuzza:** Supervision, Validation, Writing – Review & Editing, **Muayad Habashneh:** Writing – Original Draft, Investigation, Software, **Marco Domaneschi:** Supervision, Validation, Writing – Review & Editing, **Peyman Aela:** Writing – Review & Editing, Methodology, **Majid Movahedi Rad:** Conceptualization, Methodology, Software, Writing – Review & Editing, Supervision.

Disclosure statement

No potential conflict of interest was reported by the author(s).

Funding

The authors declare that they have no financial or personal relationships that may be construed as having impacted the work presented in this study.

Data availability statement

The authors confirm that the supporting data for this study's conclusions are included in the publication.

References

Bathe, K.-J. 2014. *Finite Element Procedures*. 2nd ed.

Beghini, L. L., A. Beghini, N. Katz, W. F. Baker, and G. H. Paulino. 2014. "Connecting Architecture and Engineering through Structural Topology Optimization." *Engineering Structures* 59: 716–726. https://doi.org/10.1016/j.engstruct.2013.10.032

Bendsøe, M. P. 1989. "Structural Optimization Optimal Shape Design as a Material Distribution Problem." *Structural Optimization* 1 (4): 193–202. https://doi.org/10.1007/BF01650949

Bendsøe, M. P., and O. Sigmund. 2004. *Topology Optimization*. Berlin Heidelberg: Springer.

Blachowski, B., P. Tauzowski, and J. Lógó. 2020. "Yield Limited Optimal Topology Design of Elastoplastic Structures." *Structural and Multidisciplinary Optimization* 61 (5): 1953–1976. https://doi.org/10.1007/S00158-019-02447-9/FIGURES/20

Christensen, P. W., and A. Klarbring. 2008. *An Introduction to Structural Optimization*. Springer Science & Business Media, Berlin. www.springer.com/series/6557

Cucuzza, R., A. Aloisio, R. Di Bari, and M. Domaneschi. 2024. "Vulnerability Assessment and Lifecycle Analysis of an Existing Masonry Arch Bridge." *Engineering Structures* 302: 117422. https://doi.org/10.1016/j.engstruct.2023.117422

Cucuzza, R., M. Domaneschi, R. Greco, and G. C. Marano. 2023. "Numerical Models Comparison for Fluid-Viscous Dampers: Performance Investigations through Genetic Algorithm." *Computers & Structures* 288: 107122. https://doi.org/10.1016/j.compstruc.2023.107122

European Committee for Standardisation. 1993. *EN 1993-1-5: Eurocode 3: Design of Steel Structures - Part 1-5: General Rules - Plated Structural Elements*.

European Committee for Standardisation. 2005a. *EN 1993-1-1: Eurocode 3: Design of Steel Structures - Part 1-1: General Rules and Rules for Buildings*.

European Committee for Standardisation. 2005b. *EN 1993-1-8: Eurocode 3: Design of Steel Structures - Part 1-8: Design of Joints*.

Fernández, E., C. Ayas, M. Langelaar, and P. Duysinx. 2021. "Topology Optimisation for Large-Scale Additive Manufacturing: Generating Designs Tailored to the Deposition Nozzle Size." *Virtual and Physical Prototyping* 16 (2): 196–220. https://doi.org/10.1080/17452759.2021.1914893

Gao, X., L. Li, and H. Ma. 2017. "An Adaptive Continuation Method for Topology Optimization of Continuum Structures considering Buckling Constraints." *International Journal of Applied Mechanics* 09 (07): 1750092. https://doi.org/10.1142/S1758825117500922

Habashneh, M., and M. Movahedi Rad. 2024a. "Optimizing Structural Topology Design through Consideration of Fatigue Crack Propagation." *Computer Methods in Applied Mechanics and Engineering* 419: 116629. https://doi.org/10.1016/j.cma.2023.116629

Habashneh, M., and M. Movahedi Rad. 2024b. "Plastic-Limit Probabilistic Structural Topology Optimization of Steel Beams." *Applied Mathematical Modelling* 128: 347–369. https://doi.org/10.1016/j.apm.2024.01.029

Habashneh, M., R. Cucuzza, M. Domaneschi, and M. Movahedi Rad. 2024. "Advanced Elasto-Plastic Topology Optimization of Steel Beams under Elevated Temperatures." *Advances in Engineering Software* 190: 103596. https://doi.org/10.1016/j.advengsoft.2024.103596

Hao, L., H. Liang, and L. Peigen. 2014. "Topology Optimization of Structures under Multiple Loading Cases with a New Compliance-Volume Product." *Engineering Optimization* 46 (6): 725–744. https://doi.org/10.1080/0305215X.2013.800054

Hsu, Y.-L. 1994. "A Review of Structural Shape Optimization." *Computers in Industry* 25 (1): 3–13. https://doi.org/10.1016/0166-3615(94)90028-0

Huang, X., and Y. M. Xie. 2007. "Convergent and Mesh-Independent Solutions for the Bi-Directional Evolutionary Structural Optimization Method." *Finite Elements in Analysis and Design* 43 (14): 1039–1049. https://doi.org/10.1016/j.finel.2007.06.006

Huang, X., and Y. M. Xie. 2010. *Evolutionary Topology Optimization of Continuum Structures: Methods and Applications*. Chichester: John Wiley & Sons.

Huang, X., Y. M. Xie, and M. C. Burry. 2007. "Advantages of Bi-Directional Evolutionary Structural Optimization (BESO) over Evolutionary Structural Optimization (ESO)." *Advances in Structural Engineering* 10 (6): 727–737. https://doi.org/10.1260/136943307783571436

Ibhadode, O., Z. Zhang, J. Sixt, K. M. Nsiempba, J. Orakwe, A. Martinez-Marchese, O. Ero, S. I. Shahabad, A. Bonakdar, and E. Toyserkani. 2023. "Topology Optimization for Metal Additive Manufacturing: Current Trends, Challenges, and Future Outlook." *Virtual and Physical Prototyping* 18 (1): e2181192. https://doi.org/10.1080/17452759.2023.2181192

Ivanyi, M., and C. C. Baniotopoulos. 2000. "Semi-Rigid Connections in Structural Steelwork." CISM International Centre for Mechanical Sciences Courses and Lectures 419. Springer-Verlag Wien, New York.

Kaliszky, S., and J. Lógó. 2003. "Layout Optimization of Rigid-Plastic Structures under High Intensity, Short-Time Dynamic Pressure." *Mechanics Based Design of Structures and Machines* 31 (2): 131–150. https://doi.org/10.1081/SME-120020288

Kingman, J. J., K. D. Tsavdaridis, and V. V. Toropov. 2015. "Applications of Topology Optimization in Structural Engineering: High-Rise Buildings and Steel Components." *Jordan Journal of Civil Engineering* 9 (3): 335–357. https://doi.org/10.14525/jjce.9.3.3076

Laghi, V., M. Palermo, M. Bruggi, G. Gasparini, and T. Trombetti. 2023. "Blended Structural Optimization for Wire-and-Arc Additively Manufactured Beams." *Progress in Additive Manufacturing* 8 (3): 381–392. https://doi.org/10.1007/s40964-022-00335-1

Lee, D. K., C. J. Yang, and U. Starossek. 2012. "Topology Design of Optimizing Material Arrangements of Beam-to-Column Connection Frames with Maximal Stiffness." *Scientia Iranica* 19 (4): 1025–1032. https://doi.org/10.1016/j.scient.2012.06.004

Lógó, J., and H. Ismail. 2020. Milestones in the 150-Year history of topology optimization: A review." *Computer Assisted Methods in Engineering and Science* 27: 97–132 https://doi.org/10.24423/cames.296

Lógó, J., S. Kaliszky, and M. Hjiaj. 2006. "A Parametric Survey of the Influence of the Semi-Rigid Connections on the Shakedown of Elasto-Plastic Frames. *Periodica Polytechnika*." *Civil Engeneering* 50 (2): 139–147.

Luo, Y., M. Zhou, M. Y. Wang, and Z. Deng. 2014. "Reliability Based Topology Optimization for Continuum Structures with Local Failure Constraints." *Computers & Structures* 143: 73–84. https://doi.org/10.1016/j.compstruc.2014.07.009

Michael, S. 2009. *ABAQUS/Standard User's Manual: Version 6.9.* Providence: University of Manchester.

Movahedi Rad, M., M. Habashneh, and J. Lógó. 2021. "Elasto-Plastic Limit Analysis of Reliability Based Geometrically Nonlinear Bi-Directional Evolutionary Topology Optimization." *Structures* 34: 1720–1733. https://doi.org/10.1016/j.istruc.2021.08.105

Movahedi Rad, M., M. Habashneh, and J. Lógó. 2023. "Reliability Based Bi-Directional Evolutionary Topology Optimization of Geometric and Material Nonlinear Analysis with Imperfections." *Computers & Structures* 287: 107120. https://doi.org/10.1016/j.compstruc.2023.107120

Pucker, T., and J. Grabe. 2011. "Structural Optimization in Geotechnical Engineering: Basics and Application." *Acta Geotechnica* 6 (1): 41–49. https://doi.org/10.1007/s11440-011-0134-7

Querin, O. M., G. P. Steven, and Y. M. Xie. 1998. "Evolutionary Structural Optimisation (ESO) Using a Bidirectional Algorithm." *Engineering Computations* 15 (8): 1031–1048. https://doi.org/10.1108/02644409810244129

Radwan, M., and B. Kövesdi. 2023. "Equivalent Geometrical Imperfections for Local and Global Interactive Buckling of Welded Rectangular Box-Section Columns." *Thin-Walled Structures* 192: 111140. https://doi.org/10.1016/j.tws.2023.111140

Ramm, E., K. Maute, and S. Schwarz. 1998. "Adaptive Topology and Shape Optimization." *Computational Mechanics, New Trends and Applications,* Barcelona, Spain: 1–22.

Ribeiro, T., L. Bernardo, R. Carrazedo, and D. De Domenico. 2022. "Eurocode-Compliant Topology Optimisation of Steel Moment Splice Connections." *Journal of Building Engineering* 62: 105346. https://doi.org/10.1016/j.jobe.2022.105346

Rocha, K. M., Burgos, R. B. Silva, A. T. da, and Pereira, A. 2023. "Numerical Investigation of Steel Beams with Web Openings Obtained from Topology Optimisation." *Structures* 58: 105595. https://doi.org/10.1016/j.istruc.2023.105595

Rozvany, G. I. N., O. M. Querin, and J. Lógó. 2004. *Sequential Element Rejections and Admissions (SERA) Method: Application to Multiconstraint Problems*. 10th AIAA/ISSMO Multidisciplinary Analysis and Optimization Conference, Albany, New York. https://doi.org/10.2514/6.2004-4523.

Rozvany, G. I. N., and Lewiński, T. 2014. "Topology Optimization in Structural and Continuum Mechanics International Centre for Mechanical Sciences." In CISM International Centre for Mechanical Sciences Courses and Lectures. Vol. 549. Springer, Vienna. www.springer.com/series/76

Schillo, N., and M. Feldmann. 2018. "Interaction of Local and Global Buckling of Box Sections Made of High Strength Steel." *Thin-Walled Structures* 128: 126–140. https://doi.org/10.1016/j.tws.2017.07.009

Shea, K., and I. F. C. Smith. 2006. "Improving Full-Scale Transmission Tower Design through Topology and Shape Optimization." *Journal of Structural Engineering* 132 (5): 781–790. https://doi.org/10.1061/ASCE0733-94452006132:5781

Torii, A. J., R. H. Lopez, and F. Biondini. 2012. "An Approach to Reliability-Based Shape and Topology Optimization of Truss Structures." *Engineering Optimization* 44 (1): 37–53. https://doi.org/10.1080/0305215X.2011.558578

Tsavdaridis, K. D., J. J. Kingman, and V. V. Toropov. 2015. "Application of Structural Topology Optimisation to Perforated Steel Beams." *Computers & Structures* 158: 108–123. https://doi.org/10.1016/j.compstruc.2015.05.004

Xie, Y. M., and G. P. Steven. 1993. "A Simple Evolutionary Procedure for Structural Optimization." *Compurers & Srrvcrures* 49 (5): 896.

Yang, B., and K. H. Tan. 2013. "Experimental Tests of Different Types of Bolted Steel Beam-Column Joints under a Central-Column-Removal Scenario." *Engineering Structures* 54: 112–130. https://doi.org/10.1016/j.engstruct.2013.03.037

Yang, X. Y., Y. M. Xie, G. P. Steven, and O. M. Querin. 1999. "Bidirectional Evolutionary Method for Stiffness Optimization." *AIAA Journal* 37 (11): 1483–1488. https://doi.org/10.2514/2.626